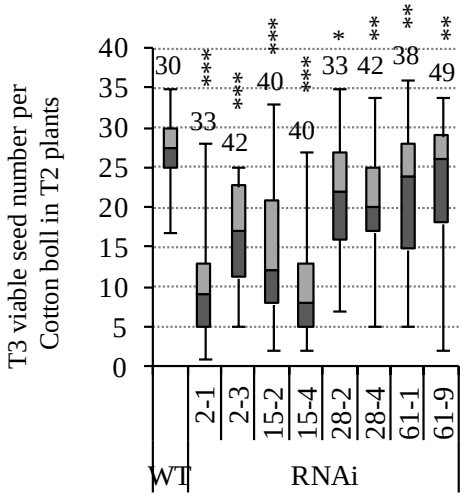

Figure S1. *GhVIN1*-RNAi cotton plants showed reduced viable seeds at T2 generation, in comparison with that in WT. Data is presented in box plots where the horizontal line within the box represents the median, while the top and bottom lines of the box represent viable seed number in 75% and 25 % of the boll population, respectively. The extent of the vertical line indicates the maximum and minimum of the data. The boll numbers used in the survey, harvested from at least 6 individual plants of each line, are indicated above the box plots. Asterisks indicate significant differences between WT and RNAi (one-way ANOVA; *, $p<0.05$; **, $p<0.01$; ***, $p<0.001$).

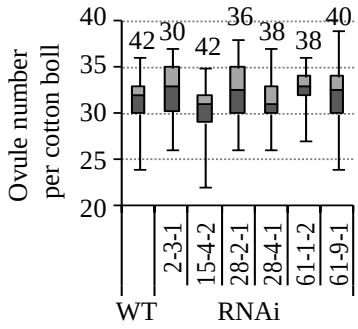

Figure S2. *GhVIN1*-RNAi cotton plants displayed ovule number per boll identical to that in WT. Data were presented in box plots as explained in Figure S1. Ovules were counted from cotton bolls harvested from 8 T_3 individuals of each line at ~3 months after germination from two independent trials. The number of cotton bolls used in each line was listed above each of the box plots, Asterisks indicate significant differences between WT and RNAi (one-way ANOVA; *, $p<0.05$; **, $p<0.01$; ***, $p<0.001$).

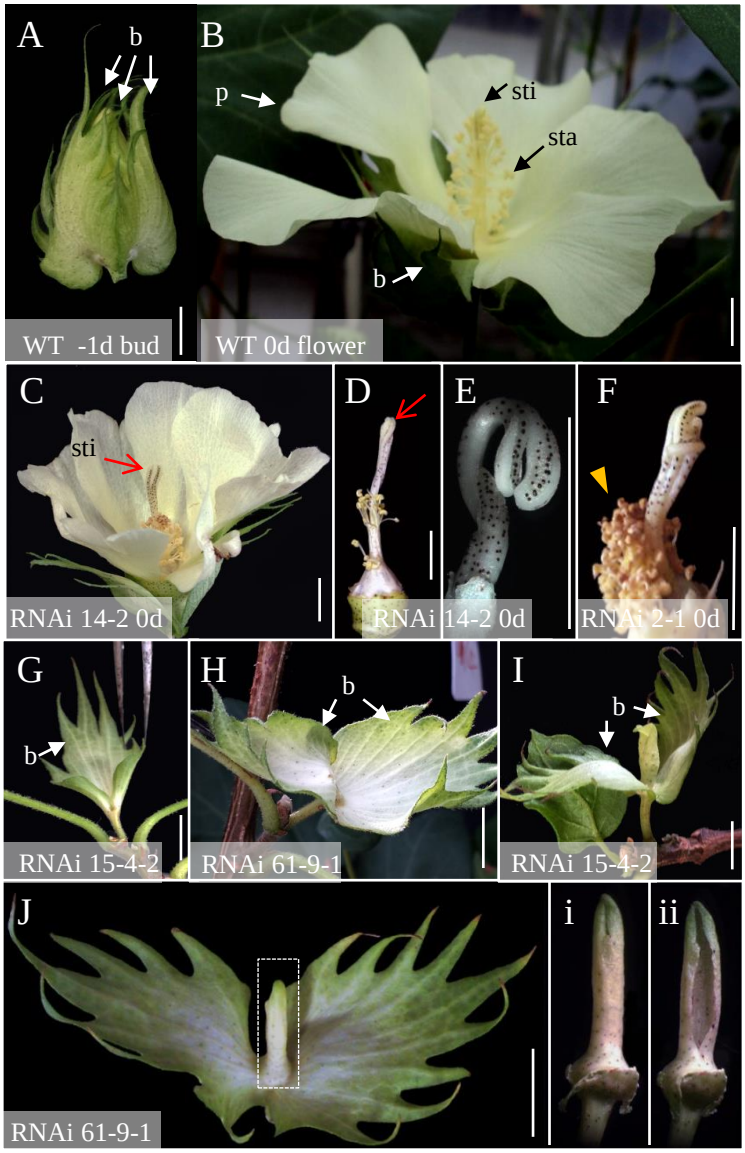

Figure S3. Suppression of *GhVIN1* affected floral organs formation.
(**A**-**B**) WT -1d bud surrounded by three bracts in a pyramid-like shape (**A**), and flower on the day of anthesis, with stigma encircled by stamen (**B**).
(**C**-**F**) RNAi cotton 0d flowers showed over-protrusion of stigma (red arrows in **C** and **D**), or malformed stigma (**E** and **F**), and significantly fewer stamen (**D**) and brown and indehiscent anthers (yellow arrowhead in **F**).
(**G**-**J**) Other severe defective floral structure phenotypes exhibited in the transgenic lines include single (**G**) and double bracts (**H**) without any other floral organs, or bracts with a tubular leafy structure in the center (**I** and **J**), instead of male and female reproductive organs. The boxed tubular structure in (**J**) is enlarged (**i**) and cut open in (**ii**).
b, bracts; p, petal; sta, stamen; sti, stigma. Bars = 1cm.

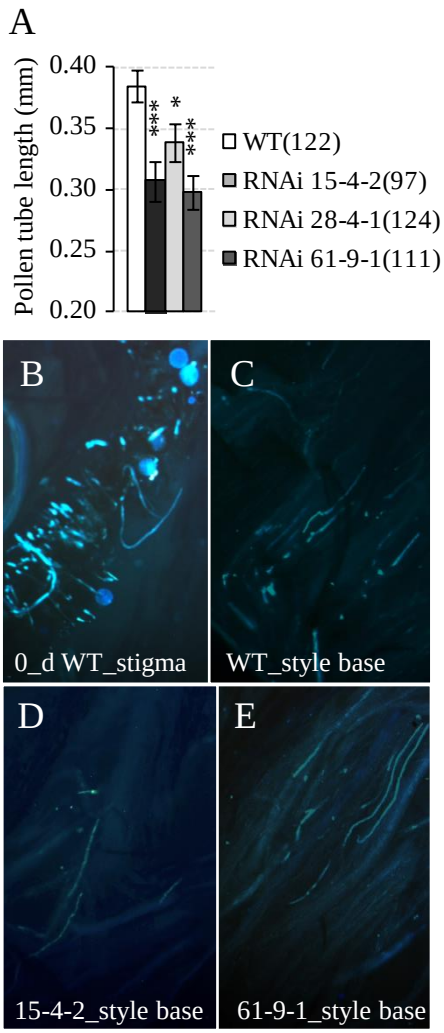

Figure S4. *In vitro* (**A**) and *in vivo* (**B**-**E**) pollen tube elongation in *GhVINs*-RNAi and WT cotton plants.

(**A**) Pollen tube length was significantly reduced after *in vitro* culture for 2 hrs. Each value is the mean ± SE of the numbers of pollen tubes listed after each genotype, collected from 8 flowers on 4 plants for each line. Asterisks indicate significant differences (Student's t-test; *, $p<0.05$; **, $p<0.01$; ***, $p<0.001$) between RNAi and WT.

(**B**-**E**) Aniline blue staining detected signals of pollen grain germination in 0_d WT stigma (**B**) and pollen tubes at the base of 1d styles in WT (**C**) and RNAi 15-4-2 (**D**) and 61-9-1 (**E**). Bar= in (**B**). The scales in (**C**-**E**) are the same as that in (**B**).

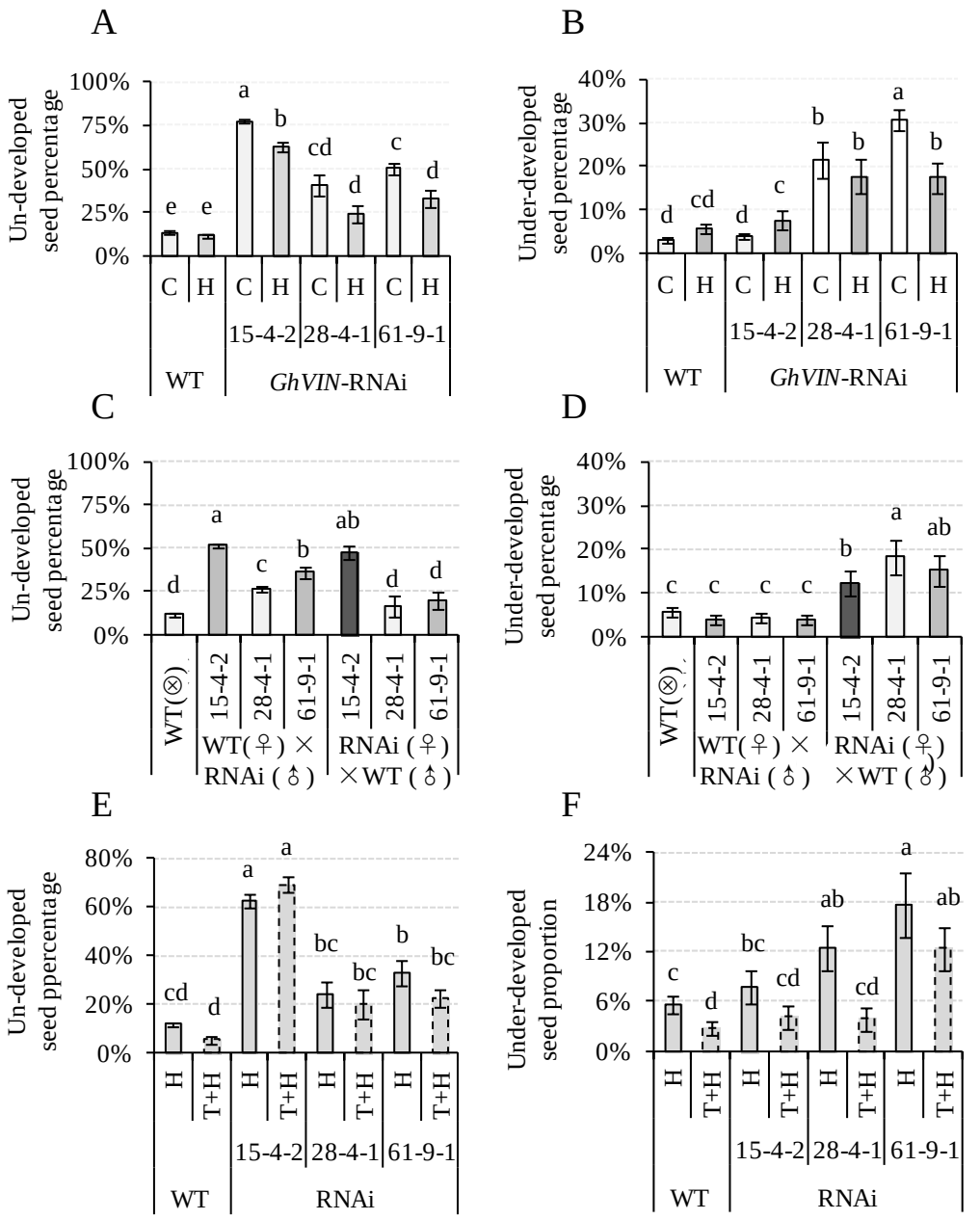

Figure S5. The percentages of un-developed seeds (**A**, **C** and **E**) and under-developed seeds (**B**, **D** and **F**) after hand pollination (**A**-**B**), reciprocal crossing (**C**-**D**), and bud thinning(**E**-**F**). C, non-treated control; H, hand pollinated bolls; T+H, bud thinning and hand pollination. Each value is the GLMM estimated mean ± SE. Data were collected from at least 20 bolls from at least 5 individual plants for each line. Different letters indicate significant difference at $p<0.05$ according to GLMM.

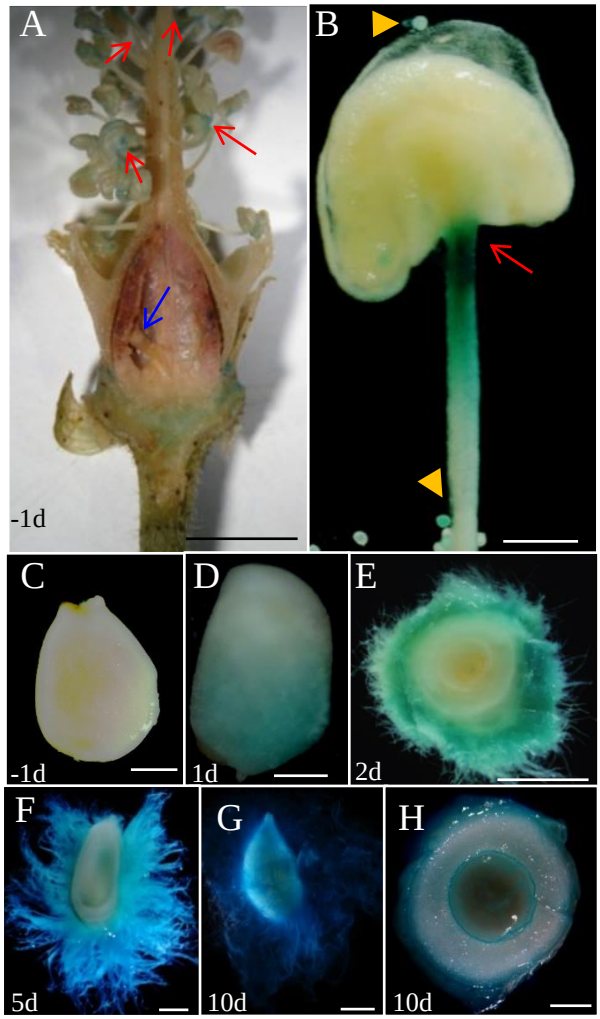

Figure S6. *RDLp::GUS* expression in -1 d transgenic cotton floral organ (**A**), stamen (**B**) and ovule (**C**), and transgenic seeds at 1 d (**D**), 2 d (**E**), 5 d (**F**), and 10 d (**G** and **H**). Red arrows in A and B indicate GUS signal in the filament and anther joint region. Yellow arrows in B show GUS in in pollen grains. Also note, no GUS signal was detected in -1d ovules (**C** and blue arrow in **A**). Bar = 5 mm in (**A**), 500 μm in (**B**-**F**), 2 mm in (**G**-**H**).

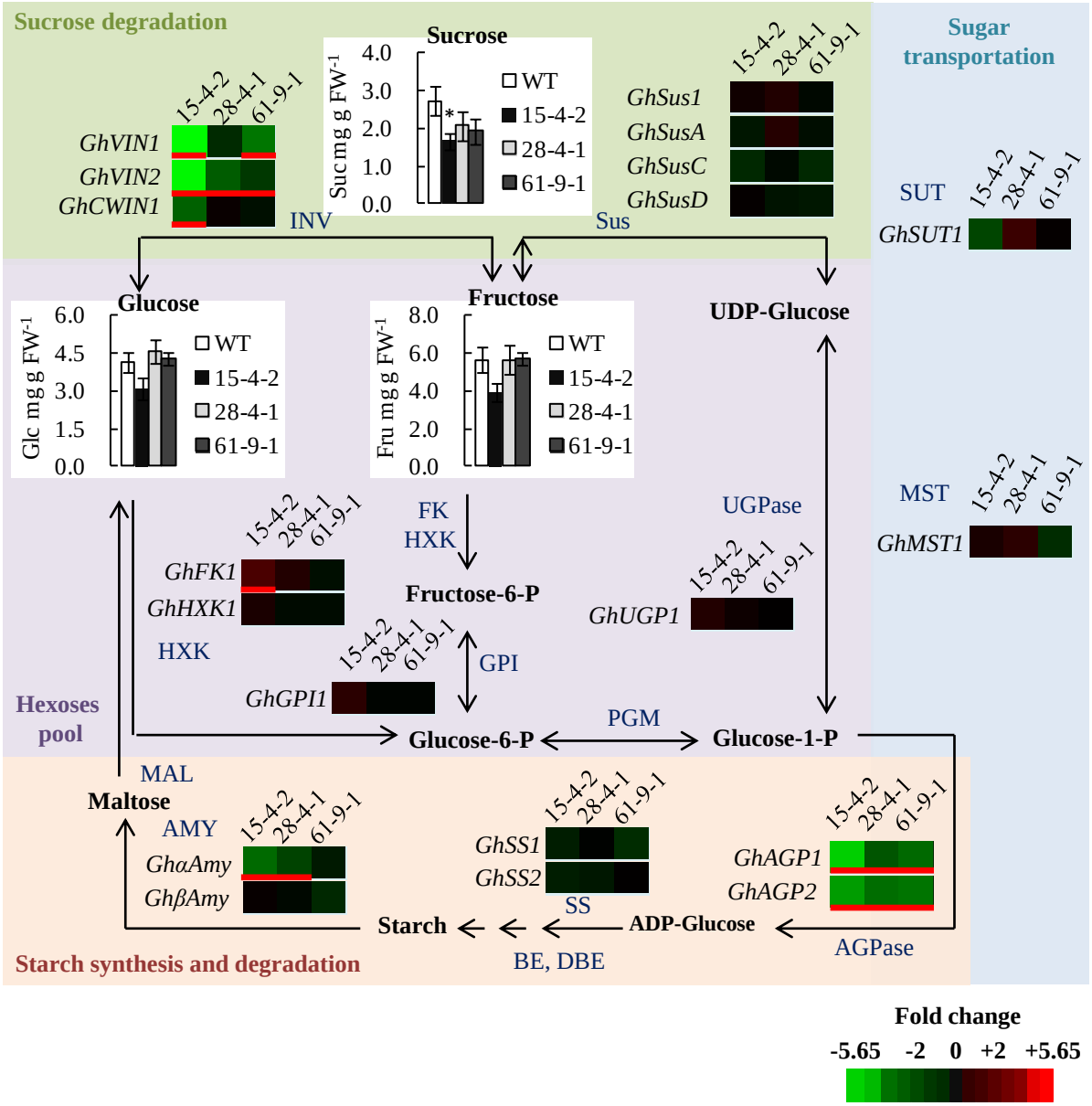

Figure S7.. A heat map of genes involved in aspects of sugar metabolism and measured soluble sugar levels in -1 d WT and RNAi stamen.

Data represent mean values ± SE ($n \geq 8$) in sugar assay. Heat map were generated according to the fold changes of qPCR mean value in each RNAi line compared to that in WT ($n \geq 6$), data were generated use the same biological replicates as in Figure 6E. Asterisks and red underlines indicate significant differences (one-way ANOVA, all pairs Turky HSD; *, $p<0.05$) between RNAi and WT. AGPase, ADP-glucose pyrophosphorylase; AMY, amylase; BE, starch branching enzyme; DBE, starch debranching enzyme; FK, fructose kinase; GPI, glucose phosphate isomerase; HXK, hexose kinase; INV, invertase; MAL, maltose; MST, monosaccharide transporter; PGM, Phosphoglucomutase; SS, starch synthase; Sus, sucrose synthase; SUT, sucrose transporter; UGPase, UDP-glucose pyrophosphorylase.

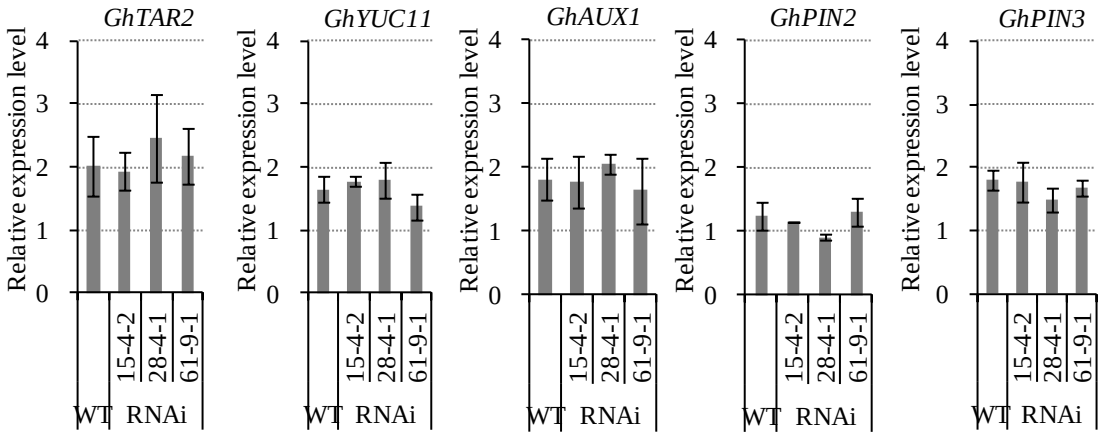

Figure S8. qPCR analysis of the transcript levels of auxin biosynthesis genes *GhTAR2* and *GhYUC11*, and auxin transportation genes *GhAUX1*, *GhPIN2* and *GhPIN3* in -1 DAA stamen from WT and RNAi plants. Data represent mean values ± SE ($n \geq 6$), from the same biological replicates as in Figure 6E. One-way ANOVA analyses (all pairs Turky HSD) showed no significant difference between WT and each RNAi line.

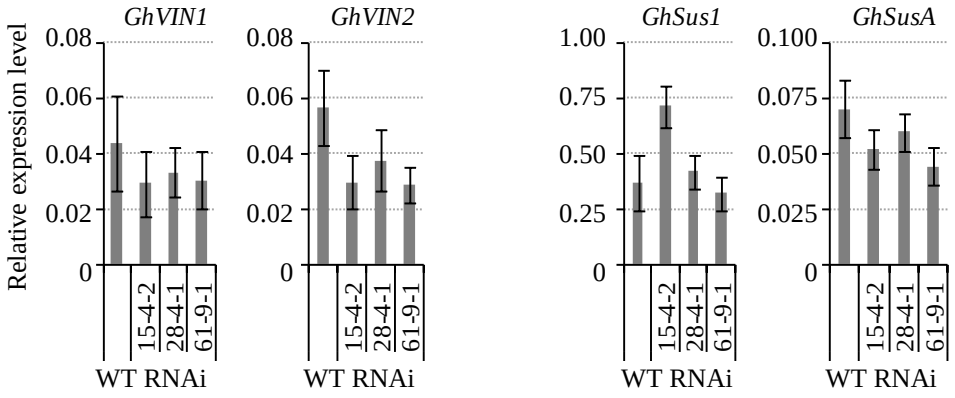

Figure S9. qPCR analysis of the transcript levels of *GhVIN1*, *GhVIN2*, *GhCWIN1*, *GhSus1* and *GhSusA* in -1 DAA styles from WT and RNAi plants. Data represent mean values ± SE ($n \geq 3$). Asterisks indicate significant differences (one-way ANOVA; *, $p<0.05$; **, $p<0.01$) between RNAi and WT.

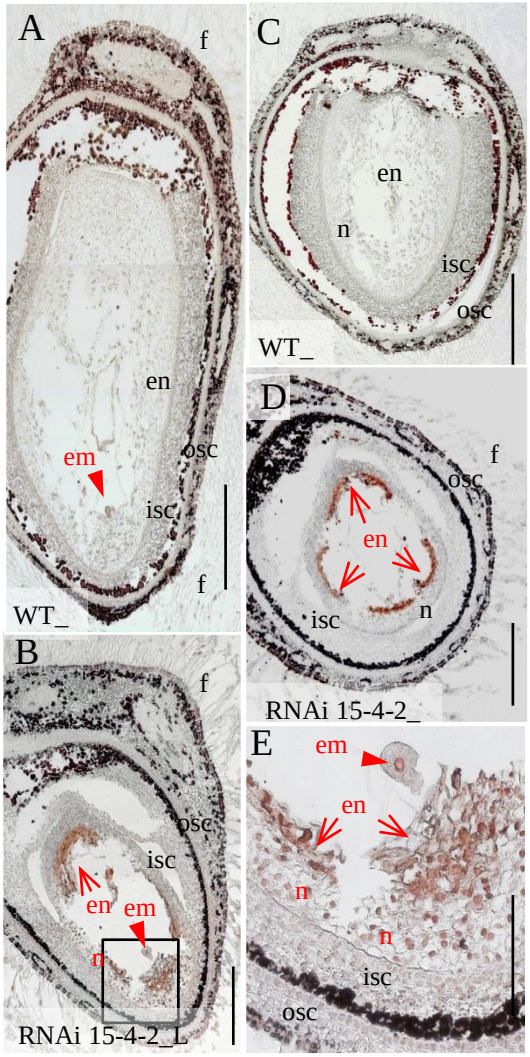

Figure S10. Colorimetric TUNEL assay on the longitudinal and cross -sections of 3d WT seed (**A** and **C**) and *GhVINs*-RNAi 15-4-2 seed (**B** and **D**), respectively. (**E**), a magnified view of the boxed regions in (**B**). Note the golden-brown TUNEL-positive signals, observed in the embryo (arrowheads), endosperm (arrows) and nucellus tissues of *GhVINs*-RNAi 15-4-2 seeds but their absence in the WT sections. em, Embryo; en, endosperm; f, fiber; isc, inner seed coat; n, nucellus; osc, outer seed coat. Bars = 200 μm in (**A**-**B**), 50μm in (**C**-**D**), and 20μm in (**E**)

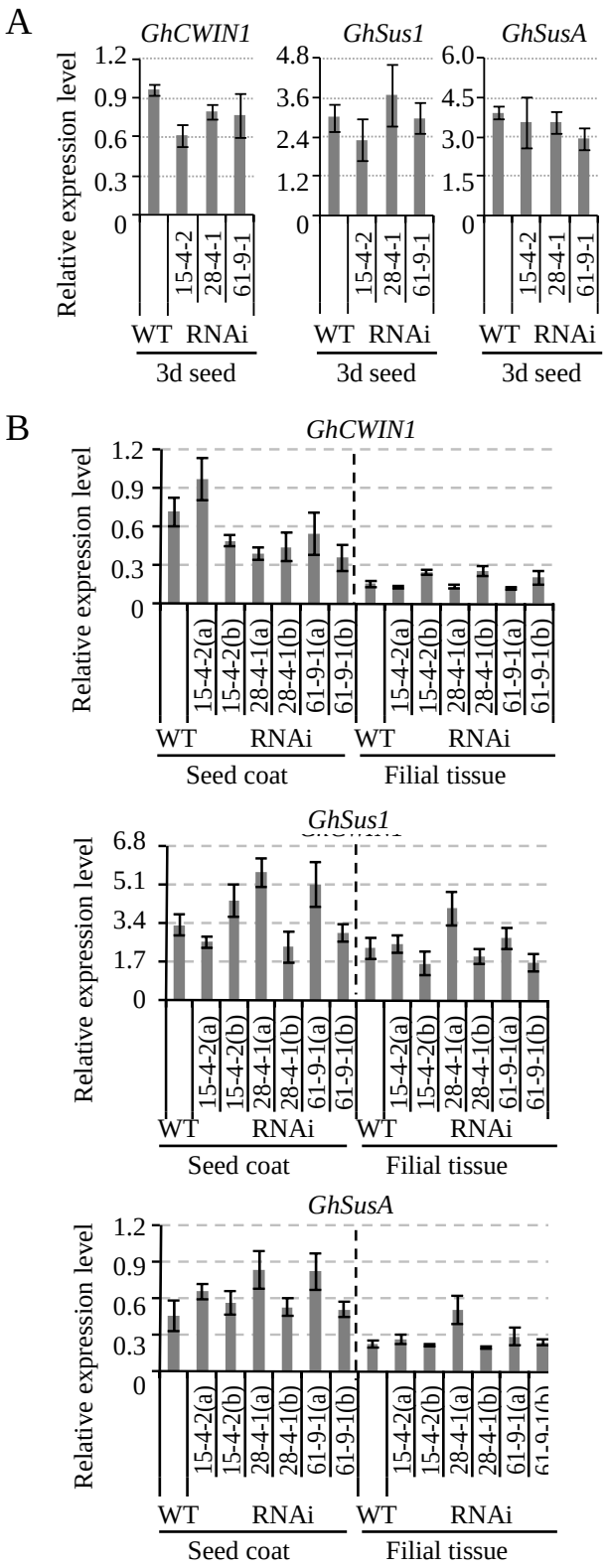

Figure S11. qPCR analyses of the expressions of *GhCWIN1*, *GhSus1* and *GhSusA* in WT and RNAi 3d seeds (**A**) and 10d seed coat and filial tissues (**B**).

For 10-d seeds from each RNAi line, replicates a and b indicate samples with strong and weak *GhVIN1* suppression, respectively, as shown in Figure 11. Data represents mean values ± SE from six biological replicates for (**A**), and at least three biological replicates for (**B**).

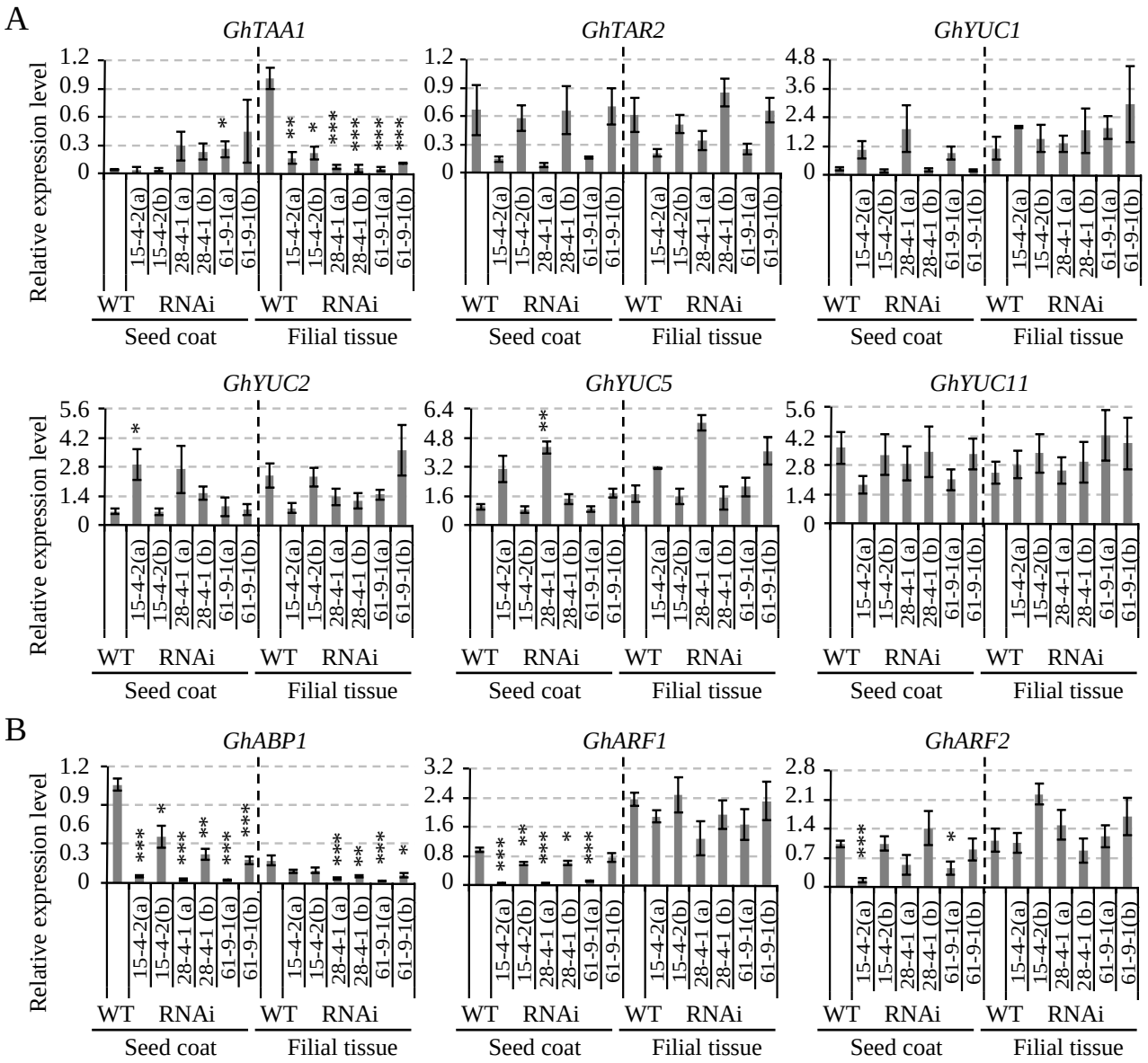

Figure S12. The expressions of genes related to auxin biosynthesis (A) and signaling response (B) were disrupted in10d WT *GhVINs*-RNAi seeds, as compare to those in WT.

For each RNAi line, replicates a and b indicate samples with strong and weak *GhVIN1* suppression, respectively, as shown in Figure 11

Data represent mean values ± SE of at least three biological samples. Asterisks indicate significant differences (one-way ANOVA; *, $p<0.05$; **, $p<0.01$; ***, $p<0.001$) between RNAi and WT.